Morphological comparison and gonadotropins cell localization of mature female turbot and mouse pituitary*

Yudong JIA[1, **], Yunhong GAO[1], Jinxing LIN[2, **]

[1] Yellow Sea Fisheries Research Institute, Chinese Academy of Fishery Sciences, Qingdao 266071, China
[2] Shanghai Laboratory Animal Research Center, Shanghai 201203, China

Abstract   Reproduction is subtlety regulated by the hypothalamic-pituitary-gonad (HPG) axis in vertebrates. Pituitary gland is the center of the HPG axis, while pituitary gonadotropins follicle stimulating hormone (FSH) and luteinizing hormone (LH) were identified the key elements of the HPG axis in teleost and mammal. Morphology, cell lines, and gonadotropins cell localization of female turbot and mouse pituitary were determined at mature stage to illustrate the anatomical difference and cell characteristics in this study. Results show that turbot pituitary is chicken heart-shaped, dorsoventral, located on the ventral surface of the diencephalon. The mouse pituitary is oval, located in the pituitary fossa of the sella turcica at the skull base. Two well-distinguished areas adenohypophysis (AH) and neurohypophysis (NH) in pituitary were identified in turbot and mouse. Turbot AH comprised the rostral pars distalis (RPD), proximal pars distalis (PPD), and pars intermedia (PI). NH was not pronounced and with finger-like protrusions into PPD. However, mouse AH only comprised the pars distalis (PD) and PI. NH distribution was semicircular. Three main types of cells (acidophilic, basophilic, and chromophobic cells) were distributed in the mouse PD region, whereas appeared in the turbot PPD, RPD, and PI. Moreover, the percentage of mouse chromophobic and basophilic cells was higher and lower than that of turbot, respectively. The diameter of the aforementioned three cells in the mouse was significantly higher than turbot. *fshβ*- and *lhβ*-immunoreactive signals were identified in turbot-distinct pituitary cells that primarily occupied the peripheral and central regions of AH. However, mouse *fsh*- and *lh*-immunoreactive cells were expressed in the same cells and present in the PD. These results demonstrate the significantly difference of pituitary morphology, cell lines and gonadotropins (*fshβ* and *lhβ*) location in female turbot and mouse. These differences help for fully understand the evolution and endocrinological functions of pituitary.

Keyword: turbot; mouse; pituitary gland; cell line; gonadotropins

1 INTRODUCTION

The pituitary is a master endocrine organ that produces and secretes 8–10 hormones from specific cell types. These hormones constitute an interface between the hypothalamus and peripheral organs and are involved in the regulation of growth, development, and reproduction (Holmes and Ball, 1974). The pituitary is composed of two compartments, namely, the neurohypophysis (NH) or posterior pituitary and the adenohypophysis (AH) or anterior pituitary based on ontogeny and morphology. The AH constitutes the majority of the pituitary mass and is composed mainly of different hormone-producing cells. However, the NH comprises only the nerve terminals of neuroendocrine cells that originated in the hypothalamus and glia-like supportive cells. The hormone-producing cell types of the AH have been investigated via histochemical, ultrastructural, and immunocytochemical techniques in mammals and teleosts (Agulleiro et al., 2006;

** Corresponding authors: ydjia2011@hotmail.com; linjinxing83@163.com

Borella et al., 2009; Mollard et al., 2012; Grandi et al., 2014). In general, hormone-producing cell types are arranged in a mosaic pattern in the adult tetrapod pituitary AH. In teleosts, the pituitary is characterized by a close interdigitating neighborhood between the NH and AH (Agulleiro et al., 2006). In contrast to mammals, teleosts lack a hypothalamo-hypophyseal portal system for the transport of neurohormonal regulators. The neurosecretory terminals of the hypothalamus exert a direct control on the secretory cells of the AH (Weltzien et al., 2004). The teleost pituitary is highly compartmentalized, and each cell type is located in a designated region as compared with the mammalian pituitary, in which the endocrine cells are distributed throughout the gland (Weltzien et al., 2004, 2014). Pituitary cell lines are mainly classified into acidophilic, basophils, and chromophobic cells and distributed in the AH. Acidophilic and basophils cell mainly comprise five hormone-producing cell types (gonadotropes, thyrotropes, lactotropes, somatotropes, and corticotropes) that each secretes gonadotropins (follicle stimulating hormone FSH and luteinizing hormone LH), thyrotropin, prolactin, growth hormone, and adrenocorticotropic in the mammals' pituitary (Ooi et al., 2004). In teleost, acidophilic cells mainly include somatotroph hormone cells and prolactin hormone cells. Basophilic cells are divided into thyrotroph cells, gonadotropin hormone cells, and adrenocorticotropic hormone cells (Hong et al., 2016). Thus, pituitary morphology, cell lines, and location of hormone-producing cell types are remarkably different in teleosts and mammals.

Turbot *Scophthalmus maximus* is cultured widely in Europe and Asia because of its high commercial value and development of domestication efforts in captivity. The aquaculture production of turbot is maintained 50 000 t in China, which accounts for 80% of the cultured world's total culture output (Jia and Lei, 2019). Similar to that in mammals, pituitary gonadotropins (GtHs), FSH and LH are the key regulators of gonad development and reproduction in teleost. Different from mammals, fish FSH and LH are dimeric proteins with a common α-subunit (CGα) and a hormone-specific β-subunit (FSHβ, LHβ) (Levavi-Sivan et al., 2010). Numerous studies have identified FSHβ and LHβ involved in the regulation of oocyte maturation and ovulation in zebrafish *Danio rerio* (Zhang et al., 2015), sablefish *Anoplopoma fimbria* (Guzmán et al., 2013), sturgeon *Acipenser gueldenstaedtii* (Hurvitz et

al., 2005), European sea bass (Mazón et al., 2015), and other fish species (Levavi-Sivan et al., 2010). Our previous studies have identified turbot gonadotropins (CGα, FSHβ, and LHβ) and the functional properties of their receptors (LHR, FSHR) during the reproductive cycle and larval development (Jia et al., 2014, 2016; Gao et al., 2019). However, in terms of turbot pituitary morphology and gonadotropin location remained unknown. The mouse is the representative mammalian model species that is widely used in scientific research. Detailed information about pituitary morphology and physiological function in mammals, including mouse have been wildly described (Amar and Weiss, 2003; Ooi et al., 2004; Hong et al., 2016). Up to now, few literatures reported the detailed information about the comprehensive compared the differences between the pituitary anatomy of reared marine fish and mammal. Elaborating the defined morphological information of the pituitary in teleost fish, and exploring the difference in the pituitaries of turbot and mouse will enrich the knowledge on vertebrate pituitary histology and evolutionary biology. Meanwhile, the pituitary produces gonadotropins that play key roles throughout the reproductive cycles of vertebrates, including mammals and teleost fish. Therefore, the distribution pattern of cells (acidophilic, basophils, chromophobic cells) and the gonadotropins (FSHβ and LHβ) in the pituitary gland of turbot and mouse were analyzed by using serial sections. Special emphasis was placed on elucidating the localization sites of the gonadotropins FSHβ and LHβ in turbot and mouse pituitaries. These data will provide detailed information about the turbot pituitary morphology, gonadotropins cell localization and may help fully understand the pituitary anatomical feature and endocrinological function.

2 MATERIAL AND METHOD

2.1 Animal and sampling

Five mature female turbots (body weight 3 500–4 000 g, body length 55–57 cm) were purchased from Tianyuan Aquaculture Co., Ltd. (Yantai, China). Fish were anesthetized with 100-mg/L tricaine methane sulfonate (MS-222, Sigma, St. Louis, MO). Five turbot pituitaries (weight 8–9 mg, diameter 3–4 mm) were quickly dissected immersed in 4% paraformaldehyde and fixed for 24 h. Meanwhile, the ovaries of the turbots were collected and fixed in 4% PFA to identify the

developmental stages of oocytes based on previous study (Jia et al., 2014). The protocol for turbot was conducted in accordance with the guidelines established by the Institutional Animal Care and Use Committee (IACUC) at Yellow Sea Fisheries Research Institute, China.

Five 10-week-old female Institute of Cancer Research (ICR) mice were obtained from the Shanghai Laboratory Animal Research Center, China. The ICR mice were reared in the Shanghai Laboratory Animal Research Center under a 12-h light/12-h dark schedule, provided ample water and food in captivity. The animal study was approved by the Shanghai Laboratory Animal Research Center Committee, and the mice were maintained in accordance with the Shanghai Laboratory Animal Research Center Guidelines for the Care and Use of Laboratory Animals. Five experimental mice weighing 21.2±0.5 g were anesthetized with 1% pentobarbital sodium. Subsequently, the pituitaries and ovaries of the mice were quickly removed and immersed in 4% PFA for 24 h.

2.2 Tissue preparation, Hematoxylin-eosin and Mallory's trichrome staining

After fixation, the pituitaries of five turbots and mice were gradually dehydrated in ethanol (75%, 20 min; 85%, 30 min; 95%, 1 h; 100%, 1 h), diaphanized in xylene (10 min) and embedded in paraffin (30 min) by using an automatic processor (Lecia, Germany). Then, 5-µm thick serial sagittal-sections were obtained by slicer (Lecia, Germany). Five complete tissue sections of turbot and mouse pituitaries were taken, mounted on poly-L-lysine coated slides and dried at 37 °C, and then subjected to histochemistry reactions. Pituitaries sections were stained with Hematoxylin-eosin staining (HE) and modified Mallory's trichrome (MT) to identify pituitary regions and cell types (Bancroft and Stevens, 1982). For HE staining, sections were deparaffinized in xylene for 25 min and successively rehydrated in 100%, 95%, 80%, and 70% ethanol for 1 min. Subsequently, the slices were stained with hematoxylin for 2 min, rinsed with distilled water for 15 min, then stained with eosin for 1 min, and rinsed again with distilled water for 10 min. Finally, the slides were dehydrated successively with 95% and 100% ethanol followed by xylene for 25 min and mounted with coverslips. For MT staining, the sections were rinsed with distilled water for 2 min, and then stained with azocarmine for 5 h. After the sections had cooled, rinsed them in distilled water,

rinsed with 1% anline in 95% alcohol for 30 s, rinsed with 5% phosphotungstic acid solution for 4 min, rinsed with the counterstain for 45 min, and finally rinsed with 95% ethanol for 1 min. The slides were then dehydrated with 95% and 100% ethanol successively followed by xylene and mounted with coverslips.

Fixed turbot and mouse ovaries were dehydrated, sliced, and stained with HE via steps similar to those above described. The pituitary and oocyte morphologies of turbots and mice were observed by using a DP72 microscope (Olympus, Tokyo, Japan). The developmental stages of turbot oocyte were identified according to our previous study (Jia et al., 2014). Briefly, the previtellogenesis stage was characterized by oocyte growth, enlargement of the nucleus (germinal vesicle), and appearance of multiple nucleoli at the periphery of the nucleus. The early vitellogenesis stage was characterized by the centralized appearance of spherical, eosinophilic, and vitellogenic yolk granules/globules in the oocyte cells. The late vitellogenesis stage was characterized by an increasing accumulation of vitellogenic granules in the oocytes and the start of the nucleic migration toward the periphery of the cell. The migratory nucleus stage, vitellogenesis reached its peak, the cell became larger and more hydrated, and the nucleus migrated toward the periphery of the cell and was in the process of dissolution. The oocytes shrunk or collapse during the atresia stage.

2.3 In-situ hybridization (ISH) and immunohistochemistry (IHC) analysis for gonadotropins

The fixation of turbot and mouse pituitaries were dehydrated, embedded into paraffin, and processed for serial paraffin sectioning at 5-µm thickness based on aforementioned method. Turbot lack of specific gonadotropins antibody. Thus, the cell location of gonadotropins in turbot and mouse pituitary were determined via ISH and IHC methods, respectively. The protocol as follows:

ISH was performed to confirm the location of pituitary gonadotropins in turbot according to the previous studies with minor modifications (Kasper et al., 2006; Chen and Ge, 2012). The probes of turbot sense and antisense digoxigenin (DIG)-labeled RNA strands were transcribed in vitro from linearized *fshβ* and *lhβ* cDNA plasmids by using a DIG RNA-labeling kit (Thermo, China). The probe sequence is listed in the Supplementary Table S1. The slides of

turbot pituitaries were deparaffinized, rehydrated, and digested by 4-µg/mL proteinase K at 37 °C for 15–20 min, followed by hybridization with DIG-labeled RNA probes at 60 °C for 12 h or overnight. The sections were washed with saline-sodium citrate for 30 min and test the hybridization signal via a TSA Plus Fluorescein/cy5/TMR System (PerkinElmer, Waltham, MA). The signal was examined by using horseradish peroxidase (HRP)-conjugated anti-fluorescein antibody with TSA Fluorescein based on the instructions of commercial kit (Roche). Without the addition of RNA probes as negative controls for ISH (Supplementary Fig.S1).

IHC was performed to identify the location of mouse pituitary gonadotropins *fsh* and *lh*. The slides of mouse pituitaries were deparaffinized, rehydrated and incubated for 20 min with blocking buffer (phosphate-buffered saline containing 5% neonatal bovine serum), followed by incubation with a rabbit anti-*fshβ* and *lhβ* polyclonal antibody (Boster, Wuhan, China) at 4 °C for 24 h. The fluorescein isothiocyanate (FITC)-conjugated secondary antibody (Abcam, USA) were incubated at 37 °C for 30 min. The FITC-labeled *fsh*- and *lh*-activated cells were detected via a fluorescent microscope in accordance with the manufacturer's instructions.

2.4 Imaging and statistical analysis

Five images were captured per slide by using the CellSens Standard system (1 260 pixels by 960 pixels). The areas of the whole pituitary and different regions (NH; rostral pars distalis, RPD; proximal pars distalis, PPD; pars intermedia, PI) in the turbots and the mice were analyzed by means of the Image Gauge software. It has been identified that turbot gonadotropins are highly homologous to those of Atlantic halibut *Hippoglossus hippoglossus* (Gao et al., 2019). In the present study, the discriminatory criteria for turbot different regions were based on those established by a previous study on Atlantic halibut (Weltzien et al., 2003, 2014). Subsequently, the proportion of different regions in the pituitary were calculated. For different cell types (acidophilic, basophilic, and chromophobe cells), five electron micrographs chosen at random were photographed for each sample from the midsagittal sections of the pituitary gland. Diameters were measured by computer analysis with a CellSens Standard Imaging System Program. Five slides per sample were analyzed in the current study. Data analysis was conducted by one-way ANOVA followed by Duncan's multiple range test via SPSS 16.0 software. All data were presented as the mean±S. D. (standard error of the mean). Statistical significance was considered at $P<0.05$.

3 RESULT

3.1 Structural characteristics of pituitary gland in turbot and mouse

The turbot pituitary was typically chicken heart-shaped, dorsoventral, located on the ventral surface of the diencephalon, and closely connected with the hypothalamus via the pituitary stalk (Figs.1a & 2a). The mouse pituitary was located in the pituitary fossa of the sella turcica at the skull base, oval with a gray-white center, and gray-red on the sides (Figs.1b & 2b). Pituitaries are composed of two different regions, the NH and AH. The turbot NH was irregularly distributed and had finger-like protrusions into the PPD, whereas the mouse NH manifested a semicircular distribution. The turbot AH was subdivided into three lobes with different patterns following the tinctorial properties of their hormone-producing cells, namely, RPD, PPD, and PI. However, the mouse AH is characterized by a well-developed pars distalis (PD) and PI.

3.2 Cell types of NH and AH in turbot and mouse

Acidophilic, basophilic, and chromophobic cells in the pituitary were distinguished via HE and MT staining. The two types of pituitary cells named fibro pituitary cell (FPC) and granular pituitary cell (GPC) were observed in the turbot NH (Figs.1c & 2c). The NH and hypothalamus of mouse were combined and contained a large number of neuroglial cells (NC) and blood sinuses (BS) (Figs.1d & 2d). The HE-stained cytoplasm was blue-purple, elliptical, or irregular for acidophilic cells (Fig.1e & g), whereas the MT-stained acidophilic cells in turbot RPD and PPD showed a dark-red cytoplasm (Fig.2e & f). In addition, the HE-stained basophilic cells in RPD and PPD were round or elliptical, and showed blue (Fig.1f).

The MT-stained cytoplasm was blue (Fig.2e & f). The acidophilic cells of PD in mice showed eosinophilic granules in the cytoplasm with a large cell volume (Figs.1h & 2g). HE staining detected single and few basophilic blue granules in the cytoplasm of basophilic cells by HE-stained (Fig.1h), whereas the MT-stained basophilic cells of PD showed a yellow cytoplasm (Fig.2g). The cytoplasm of chromophobic cells was transparent, the envelope was not evident, the volume was
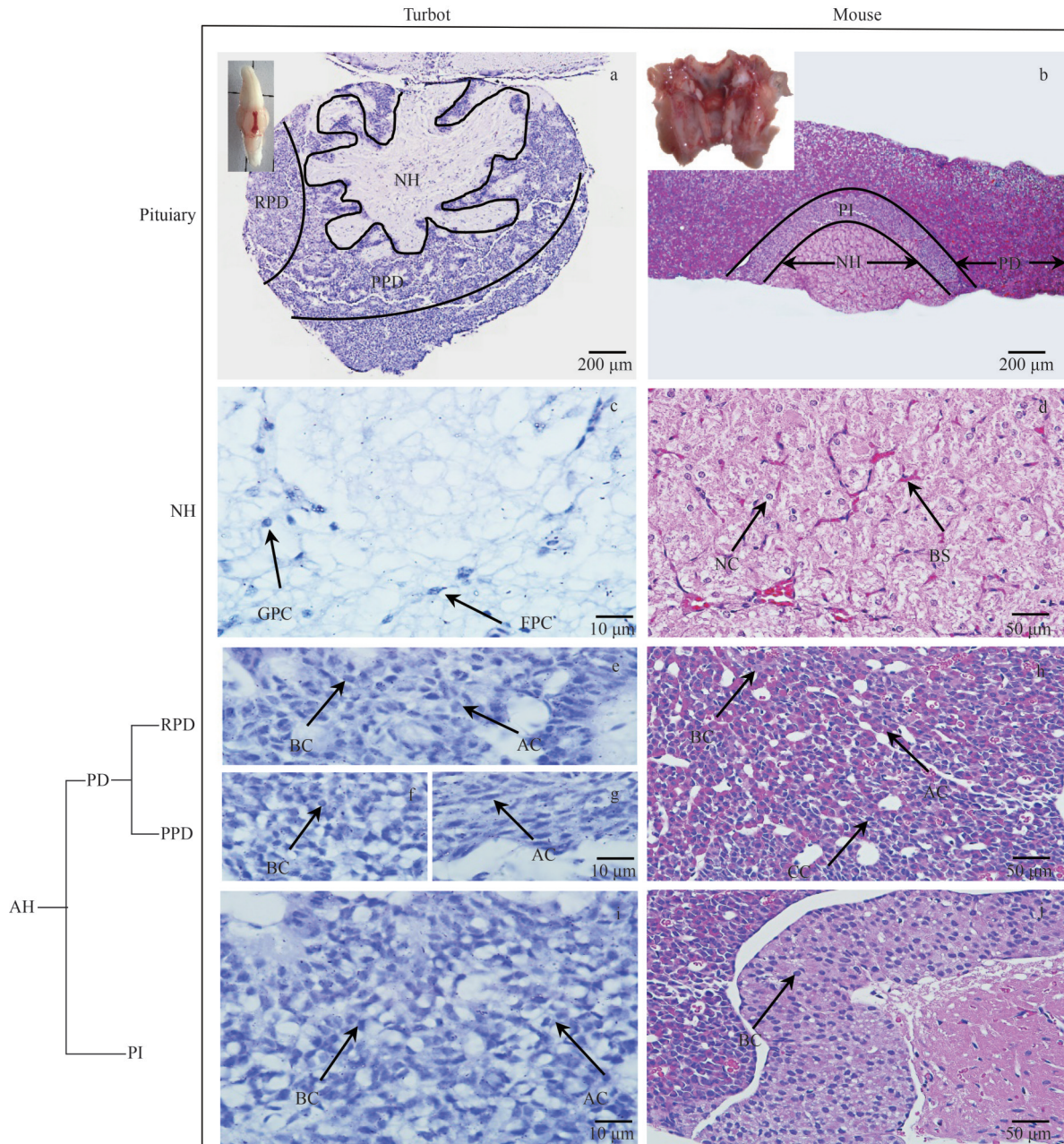
Fig.1 Structure of adult turbot and mouse pituitary stained by HE staining

AH: adenohypophysis; NH: neurohypophysis; PD: pars distals; RPD: rostral pars distalis; PPD: proximal pars distalis; PI: pars intermedia; FPC: fibro pituitary cells; GPC: granular pituitary cells; NC: neuroglial cells; BS: blood sinuses; AC: acidophilic cells; BC: basophilic cells; CC: chromophobe cells.

small, and the quantity was large in mouse (Fig.1h). In the turbot PI region, the MT-stained cytoplasm of acidophilic cells was dark red, the nucleus was light red, and the cytoplasm of basophils was light blue (Figs.1i & 2h). The mouse PI mainly comprised basophilic cells with round or polygonal hyperchromatic nuclei (Figs.1j & 2i).

The area of NH, RPD, PPD, and PI accounted for 31%, 16%, 34%, and 19% of the sagittal area of the turbot pituitary, respectively (Fig.3a). In mouse, NH accounted for about 15% of the sagittal area of pituitary gland, PI about 13%, and PD about 72% (Fig.3a). Acidophilic, basophilic, and chromophobic cells account for approximately 65%, 30%, and 5% of the turbot pituitary (Fig.3b), respectively. The percentages of acidophilic, basophilic, and chromophobic cells in the mouse pituitary gland were approximately 55%, 15%, and 30% (Fig.3b), respectively.
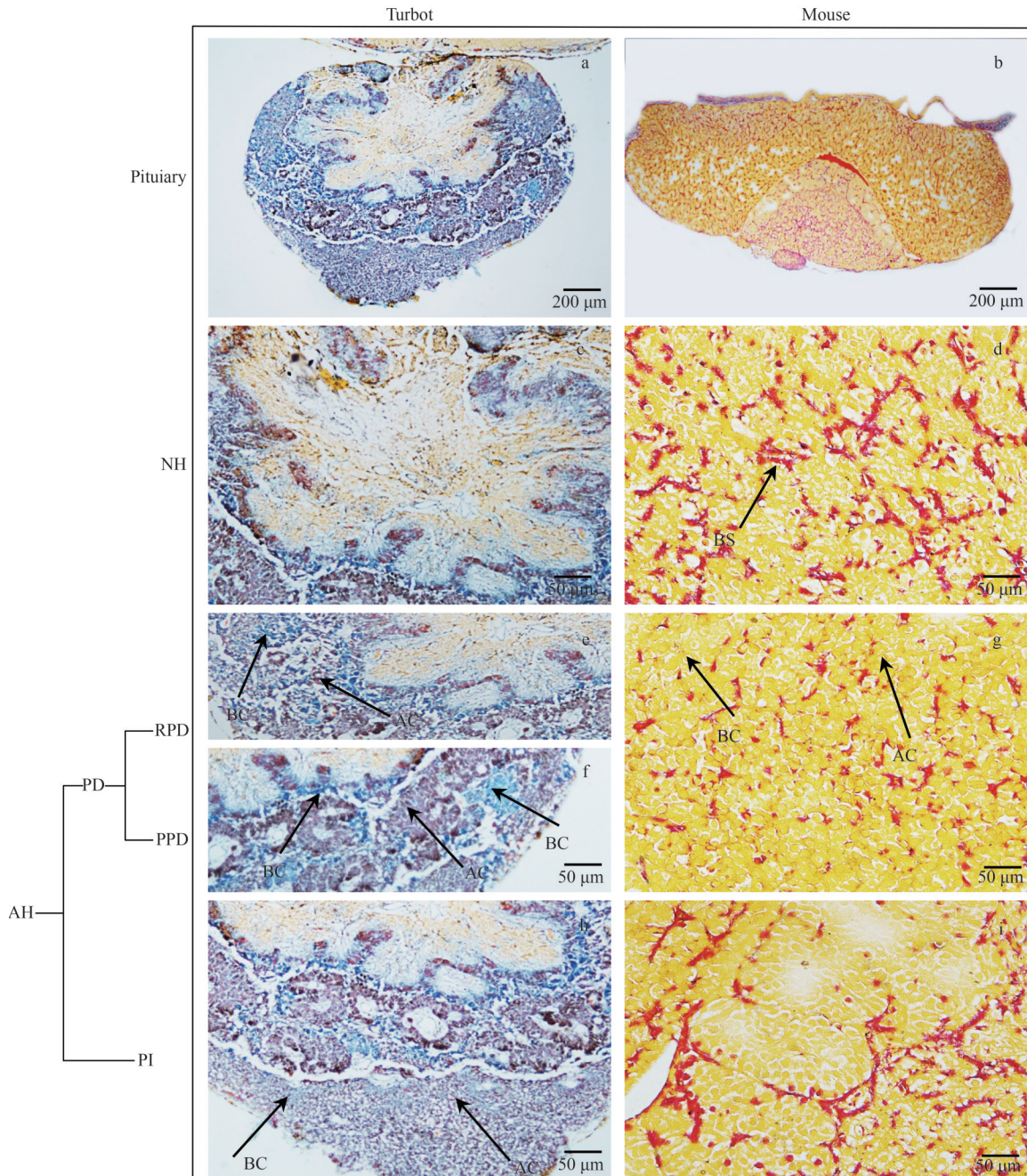
Fig.2 Cell lines of turbot and mouse pituitary via stained with modified Mallory's trichrome (MT) staining

AH: adenohypophysis; NH: neurohypophysis; PD: pars distals; RPD: rostral pars distalis; PPD: proximal pars distalis; PI: pars intermedia; BS: blood sinuses; AC: acidophilic cells; BC: basophilic cells; CC: chromophobe cells.

Significant differences in the diameters of acidophilic cells, basophilic cells, and chromophore cells were observed between the PDs of turbots and mice (Fig.4a, $P<0.05$). Similar results were found for pituitary cell diameter in the NH and basophilic cells in the PI (Fig.4b & c; $P<0.05$). In addition, the higher diameters of above three cells were observed in the mice than in the turbots (Fig.4; $P<0.05$).

3.3 Location of *fshβ* and *lhβ* in turbot and mouse pituitary

The locations of *fshβ* and *lhβ* in turbot and mouse pituitaries were evaluated via ISH and IHC analysis, respectively. Ovarian histological observation revealed that the turbots and mice were sexually mature individuals (Supplementary Fig.S2). Turbot oocytes at Latvtg stage were characterized by the increasing
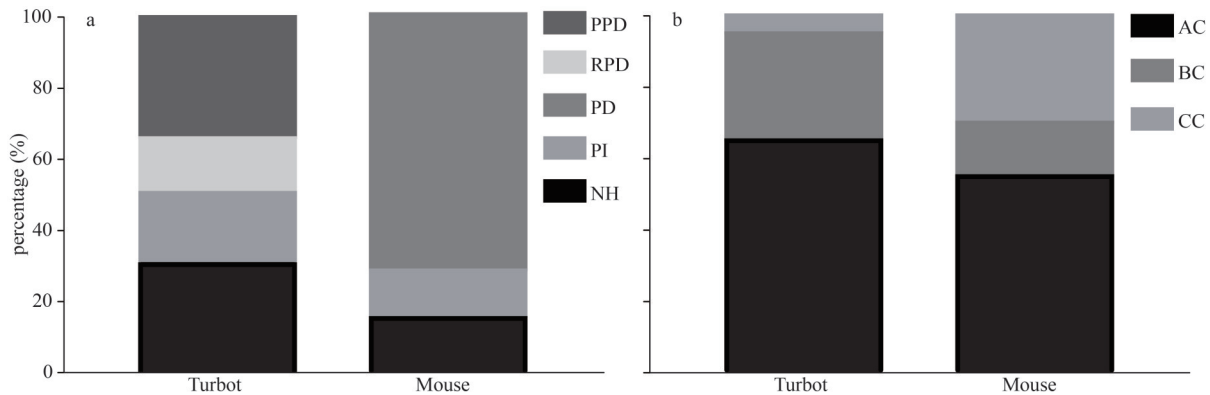
Fig.3 Percentage (a) and diameter (b) of acidophilic, basophilic, and chromophobe cells in the pituitary of turbot and mouse
PPD: proximal pars distalis; RPD: rostral pars distalis; PD: pars distals; PI: pars intermedia; NH: neurohypophysis; Data are presented as means±S.D. AC: acidophilic cells; BC: basophilic ccells; CC: chromophobic cells.
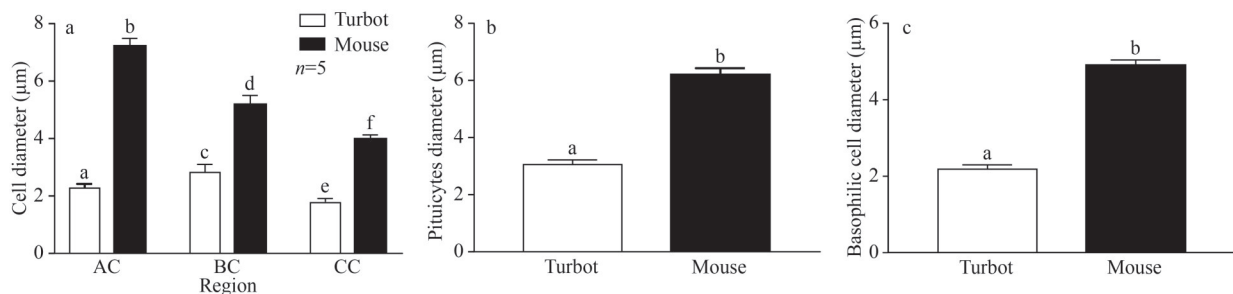

Fig.4 Diameter of different type of cells in the PD (a), NH (b), and PI (c) regions of turbot and mouse pituitary
Data are presented as means±S.D. Bars with different superscripts are statistically different ($P<0.05$, $n=5$). PD: pars distals; NH: neurohypophysis; PI: pars intermedia; AC: acidophilic cells; BC: basophilic ccells; CC: chromophobic cells.

accumulation of vitellogenic granules and the start of nucleic migration toward the cell periphery. The *fshβ* and *lhβ* of turbots were expressed in different cell types in turbot, whereas they were expressed in the same cell type in mice (Fig.5). The turbot *lhβ* cells were dispersed and located centrally, whereas some *fshβ* cells were largely located at the periphery in the AH. In mice, *fsh* and *lh* were expressed in the PD.

The diameter of turbot *fshβ* cells was significantly higher than that of turbot *lhβ* cells (Fig.6; $P<0.05$), whereas no significant difference was observed between mouse *fshβ* and *lhβ* cells (Fig.6; $P>0.05$). In addition, the diameter of *fshβ* and *lhβ* cells in mice was significantly higher than that of *fshβ* and *lhβ* cells in turbots (Fig.6; $P<0.05$).

4 DISCUSSION

In this work, the morphological differences of the pituitary and cell lines in adult female turbot and mouse were compared and the location of FSH and LH in pituitary glands was elucidated. In general, the pituitary can be divided into the NH and AH

two main compartments based on ontogeny and morphology. The turbot pituitary gland is unique in contrast to that of the mouse; its NH forms a central core that is surrounded by a superficial AH in the present study. Mammals have a well-developed AH and PD, while the PI is small or absent at the adult stage (Norris, 2007). The pituitary is characterized by a close interdigitating neighborhood between the NH and AH in fish, while the latter comprises RPD, PPD, and PI (Agulleiro et al., 2006). The turbot pituitary AH manifests a similar structure, whereas the mouse AH only includes PD and PI. In mammals the NH is located posterior to the AH, while in lower tetrapods and especially in fish, the NH is to a varying degree located dorsal to the AH (Norris, 2007). Weltzien et al. (2014) reported the PI generally makes up a large part of the pituitary, while the AH is relatively less pronounced, with finger-like protrusions into the PD and especially the PI in fish. The proportion of each component showed a significant difference in turbot and mouse. Thus, these results of the morphological differences in the pituitary demonstrated evolution difference and may cause different endocrinological regulating
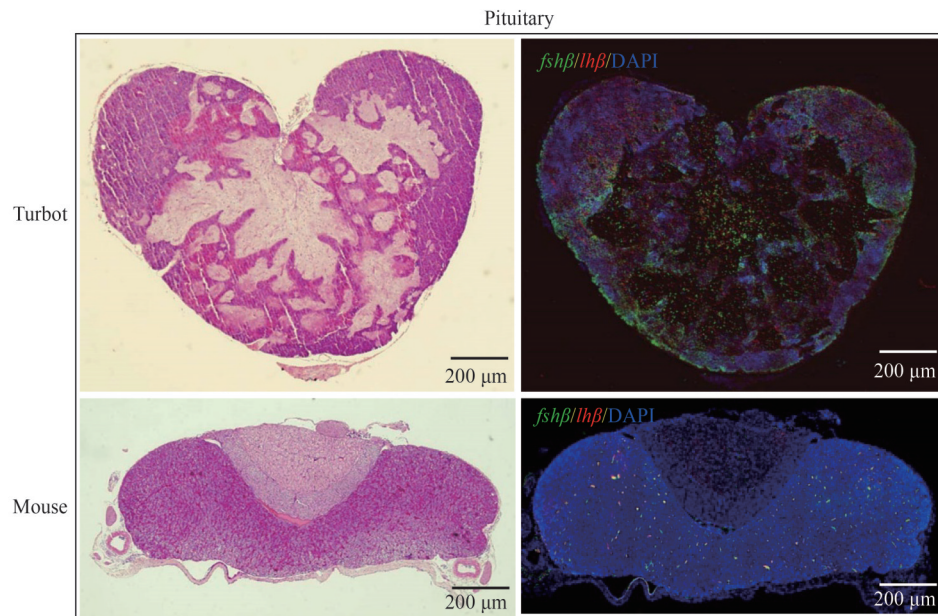
Fig.5 Location of gonadotropins in adult turbot and mouse pituitary by double-colored in-situ hybridization (ISH) (top right panel) and immunohistochemistry (IHC) (lower right panel)
Cross section stained for $fsh\beta$ (green) and $lh\beta$ (red). The nuclei were stained by 40,6-diamidino-2-phenylindole (DAPI; blue).
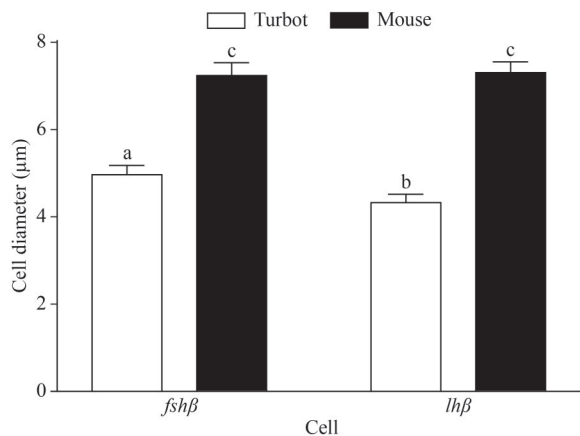

Fig.6 Diameter of gonadotropins cells ($fsh\beta$, $lh\beta$) in the pituitary of turbot and mouse
Data are presented as means±S.D. Bars with different superscripts are statistically different ($P<0.05$, $n=5$).

mechanism in mouse and turbot.

AH is composed mostly of different hormone-producing cells in vertebrates, including fish. Numerous studies have investigated the distribution patterns of the different endocrine cell types in the AH (Ooi et al., 2004; Kasper et al., 2006; El-Sakhawy et al., 2011; Chen and Ge, 2012). Kasper et al. (2006) investigated the distribution of eosinophilic and basophilic cells in the pituitary of Nile tilapia via HE staining. El-Sakhawy et al. (2011) identified the main cellular group in the Nile tilapia AH via different chemical staining methods. In addition, different endocrine cell types in AH have been reported in gobiid fish (Yoshie and Honma, 1978), zebrafish (Herzog et al., 2003; Pogoda and Hammerschmidt, 2009), cichlid fish (Mattheij et al., 1971), and other fish species (Cerdá-Reverter and Canosa, 2009). Similar studies on cell identification and distribution in the rat AH have been performed (Ifft, 1953; D'Este et al., 2005; Musumeci et al., 2015). Different cells produce different hormones and regulate distinct biological processes. In general, acidophilic cells include somatotroph and prolactin hormone cells. Basophilic cells are divided into thyrotrophic, gonadotropic, and adrenocorticotropic hormone cells, and chromophobic cells that support nutrition or phagocytosis; some chromophobic cells secrete granules that can produce adrenocorticotropic hormones (Japón et al., 1994). The prolactin and corticotropic cells are usually detected in RPD; the somatotropic, thyrotropic, and gonadotropic (FSH and LH) cells are detected in PPD; and the somatolactin, melanotropic, and endorphin cells in PI are found in numerous teleost species (Agulleiro et al., 2006; Borella et al., 2009; Cerdá-Reverter et al., 2009; Grandi et al., 2014). In the present study, the mouse pituitary acidophilic, basophilic, and chromophobic cells were distributed in the PD region, whereas these cells were observed in turbot

pituitary PPD, RPD, and PI. In addition, the percent and diameter of the three cells manifested a significant difference in mouse and turbot pituitary. The distributed differences of turbot and mouse pituitary cells manifested significantly species-specific difference and suggest these cells may play different roles during biological processes.

Reproduction in vertebrates is a complex physiological process that depends on the coordinated regulation of various hormones via endocrine, paracrine, and autocrine manners. The key modulators of reproduction are GtHs both LH and FSH, which are produced by the pituitary. The "one cell, one hormone" pituitary model assumes that each hormone is expressed by a distinct cell type (Zhu et al., 2007; Davis et al., 2016). However, GtHs (FSH and LH) exhibit significantly different cell expression profiles between mammals and fish. In mammals and many other studied tetrapods, both GtHs are produced in the same cell; by contrast, in fish, gonadotropes secrete either FSH or LH, but not both (Shimizu et al., 2003; Weltzien et al., 2014; Fontaine et al., 2020). In female zebrafish, FSH cells colocalize with LH cells in the PPD region with the former scattered individually, whereas LH cells normally form aggregates (Chen and Ge, 2012). In general, the method of ISH become effective ways to investigate the functional genes cell location due to most farming fish lack of specific antibody. Up to now, there is no specific FSHβ and LHβ antibody for turbot. In the current study, *fshβ* and *lhβ* cells were expressed in different cells in turbots, whereas they were expressed in the same cell type in mice by ISH. In addition, histological and immunohistochemical analyses indicated that *fshβ* and *lhβ* cells were widely distributed along the turbot adenohypophysis. Similar results have been reported for most other fish species (Shimizu et al., 2003; Weltzien et al., 2003, 2014; Honji et al., 2013; Golan et al., 2016; Fontaine et al., 2020). We also found the diameter of *fshβ* cells was significantly higher than *lhβ* cells in turbot pituitary, whereas no significant difference was observed in mouse in the current study. These results suggested that GtHs might present the specific mechanism involved in the regulation of reproductive processes in turbots and mice because of different cell locations.

5 CONCLUSION

These results of this study demonstrated the significantly difference of pituitary morphology, cell types and characteristics in turbot and mouse. In addition, *fshβ* and *lhβ* were found to be expressed by different cell types in the turbot pituitary, whereas they were expressed in the same cell type in the mouse pituitary. These differences reflect species differences at the pituitary anatomical level and provide basic data for studying the evolution and pituitary endocrinological regulating networks. Furthermore, the above results, together with our previous study (Jia et al., 2014, 2016; Gao et al., 2019), strengthened and revealed the endocrinological roles of turbot gonadotrophins.

6 DATA AVAILABILITY STATEMENT

The turbot *FSHβ* and *LHβ* gene sequence are is available from the National Center for Biotechnology. Information under the accession numbers KP658394.1 and MK290836.1.

References

Agulleiro B, García H M P, García A A. 2006. Teleost adenohypophysis: morphofunctional and developmental aspects. *In*: Reinecke M, Zaccone G, Kapoor B G eds. *Fish Endocrinology*. Science Publishers, Enfield. p.290-324.

Amar A P, Weiss M H. 2003. Pituitary anatomy and physiology. *Neurosurgery Clinics of North America*, **14**(1): 11-23, https://doi.org/10.1016/S1042-3680(02)00017-7.

Bancroft J D, Stevens A. 1982. Theory and Practice of Histological Techniques. 2nd edn. Churchill Livingstone, New York.

Borella M I, Venturieri R, Mancera J M. 2009. Immunocytochemical identification of adenohypophyseal cells in the pirarucu (*Arapaima gigas*), an Amazonian basal teleost. *Fish Physiology and Biochemistry*, **35**(1): 3-16, https://doi.org/10.1007/s10695-008-9254-x.

Cerdá-Reverter J M, Canosa L F. 2009. Neuroendocrine systems of the fish brain. *Fish Physiology*, **28**: 3-74, https://doi.org/10.1016/S1546-5098(09)28001-0.

Chen W T, Ge W. 2012. Ontogenic expression profiles of gonadotropins (*fshb* and *lhb*) and growth hormone (*gh*) during sexual differentiation and puberty onset in female zebrafish. *Biology of Reproduction*, **86**(3): 73, https://doi.org/10.1095/biolreprod.111.094730.

Davis S W, Keisler J L, Pérez-Millán M I et al. 2016. All hormone-producing cell types of the pituitary intermediate and anterior lobes derive from *prop1*-expressing progenitors. *Endocrinology*, **157**(4): 1385-1396, https://doi.org/10.1210/en.2015-1862.

D'Este L, Casini A, Cetin Y et al. 2005. Guanylin-immunoreactive cells in the female and male rat adenohypophysis and their changes under various physiological and experimental conditions. *Histochemistry and Cell Biology*, **123**(3): 303-313, https://doi.org/10.1007/

s00418-004-0738-1.

El-Sakhawy M A, El-Shamma M A, Rabou M I A et al. 2011. Seasonal histology and histochemistry of the adenohypophysis of *nile tilapia* (*Oreochromis niloticus*). *Journal of Veterinary Anatomy*, **4**(2): 39-60, https://doi.org/10.21608/jva.2011.45307.

Fontaine R, Ciani E, Haug T M et al. 2020. Gonadotrope plasticity at cellular, population and structural levels: a comparison between fishes and mammals. *General and Comparative Endocrinology*, **287**: 113344, https://doi.org/10.1016/j.ygcen.2019.113344

Gao Y H, Jing Q Q, Huang B et al. 2019. Molecular cloning, characterization, and mRNA expression of gonadotropins during larval development in turbot (*Scophthalmus maximus*). *Fish Physiology and Biochemistry*, **45**(5): 1697-1707, https://doi.org/10.1007/s10695-019-00656-z.

Golan M, Martin A O, Mollard P et al. 2016. Anatomical and functional gonadotrope networks in the teleost pituitary. *Scientific Reports*, **6**(1): 23777, https://doi.org/10.1038/srep23777.

Grandi G, Marchetti M G, Lanzoni M et al. 2014. Immunocytochemical and ultrastructural identification of adenohypophyseal cells in *Ctenopharyngodon idella* (Cypriniformes: Cyprinidae) during gonadal differentiation. *Fish Physiology and Biochemistry*, **40**(4): 1115-1139, https://doi.org/10.1007/s10695-014-9910-2.

Guzmán J M, Luckenbach J A, Swanson P. 2013. Molecular characterization and quantification of sablefish (*Anoplopoma fimbria*) gonadotropins and their receptors: reproductive dysfunction in female captive broodstock. *General and Comparative Endocrinology*, **193**: 37-47, https://doi.org/10.1016/j.ygcen.2013.07.007.

Herzog W, Zeng X C, Lele Z et al. 2003. Adenohypophysis formation in the zebrafish and its dependence on sonic hedgehog. *Developmental Biology*, **254**(1): 36-49, https://doi.org/10.1016/S0012-1606(02)00124-0.

Holmes R L, Ball J N. 1974. The Pituitary Gland: A Comparative Account. Cambridge University Press, London.

Hong G K, Payne S C, Jane J A Jr. 2016. Anatomy, physiology, and laboratory evaluation of the pituitary gland. *Otolaryngologic Clinics of North America*, **49**(1): 21-32, https://doi.org/10.1016/j.otc.2015.09.002.

Honji R M, Nóbrega R H, Pandolfi M et al. 2013. Immunohistochemical study of pituitary cells in wild and captive *salminus hilarii* (*characiformes*: *characidae*) females during the annual reproductive cycle. *SpringerPlus*, **2**(1): 460, https://doi.org/10.1186/2193-1801-2-460.

Hurvitz A, Degani G, Goldberg D et al. 2005. Cloning of FSHβ, LHβ, and glycoprotein α subunits from the Russian Sturgeon (*Acipenser gueldenstaedtii*), β-subunit mRNA expression, gonad development, and steroid levels in immature fish. *General and Comparative Endocrinology*, **140**(1): 61-73, https://doi.org/10.1016/j.ygcen.2004.09.019.

Ifft J D. 1953. The effect of superior cervical ganglionectomy on the cell population of the rat adenohypophysis and on the estrous cycle. *The Anatomical Record*, **117**(3): 395-404, https://doi.org/10.1002/ar.1091170305.

Japón M A, Rubinstein M, Low M J. 1994. In situ hybridization analysis of anterior pituitary hormone gene expression during fetal mouse development. *Journal of Histochemistry & Cytochemistry*, **42**(8): 1117-1125, https://doi.org/10.1177/42.8.8027530.

Jia Y D, Lei J L. 2019. Molecular function of gonadotrophins and their receptors in the ovarian development of turbot (*Scophthalmus maximus*). *General and Comparative Endocrinology*, **277**: 17-19, https://doi.org/10.1016/j.ygcen.2019.02.014.

Jia Y D, Meng Z, Niu H X et al. 2014. Molecular cloning, characterization, and expression analysis of luteinizing hormone receptor gene in turbot (*Scophthalmus maximus*). *Fish Physiology and Biochemistry*, **40**(6): 1639-1650, https://doi.org/10.1007/s10695-014-9954-3.

Jia Y D, Sun A, Meng Z et al. 2016. Molecular characterization and quantification of the follicle-stimulating hormone receptor in turbot (*Scophthalmus maximus*). *Fish Physiology and Biochemistry*, **42**(1): 179-191, https://doi.org/10.1007/s10695-015-0128-8.

Kasper R S, Shved N, Takahashi A et al. 2006. A systematic immunohistochemical survey of the distribution patterns of GH, prolactin, somatolactin, β-TSH, β-FSH, β-LH, ACTH, and α-MSH in the adenohypophysis of *Oreochromis niloticus*, the Nile tilapia. *Cell and Tissue Research*, **325**(2): 303-313, https://doi.org/10.1007/s00441-005-0119-7.

Levavi-Sivan B, Bogerd J, Mañanós E L et al. 2010. Perspectives on fish gonadotropins and their receptors. *General and Comparative Endocrinology*, **165**(3): 412-437, https://doi.org/10.1016/j.ygcen.2009.07.019.

Mattheij J A M, Stroband H W J, Kingma F J. 1971. The cell types in the adenohypophysis of the cichlid fish *Cichlasoma biocellatum* regan, with special attention to its osmoregulatory role. *Zeitschrift für Zellforschung und mikroskopische Anatomie*, **118**(1): 113-126, https://doi.org/10.1007/BF00331770.

Mazón M J, Molés G, Rocha A et al. 2015. Gonadotropins in European sea bass: endocrine roles and biotechnological applications. *General and Comparative Endocrinology*, **221**: 31-41, https://doi.org/10.1016/j.ygcen.2015.05.002.

Mollard P, Hodson D J, Lafont C et al. 2012. A tridimensional view of pituitary development and function. *Trends in Endocrinology & Metabolism*, **23**(6): 261-269, https://doi.org/10.1016/j.tem.2012.02.004.

Musumeci G, Castorina S, Castrogiovanni P et al. 2015. A journey through the pituitary gland: development, structure and function, with emphasis on embryo-foetal and later development. *Acta Histochemica*, **117**(4-5): 355-366, https://doi.org/10.1016/j.acthis.2015.02.008.

Norris D O. 2007. Vertebrate Endocrinology, 4th edn. Academic Press. p.549.

Ooi G T, Tawadros N, Escalona R M. 2004. Pituitary cell lines and their endocrine applications. *Molecular and Cellular Endocrinology*, **228**(1-2): 1-21, https://doi.org/10.1016/j.mce.2004.07.018.

Pogoda H M, Hammerschmidt M. 2009. How to make a teleost adenohypophysis: molecular pathways of pituitary development in zebrafish. *Molecular and Cellular Endocrinology*, **312**(1-2): 2-13, https://doi.org/10.1016/j.mce.2009.03.012.

Shimizu A, Tanaka H, Kagawa H. 2003. Immunocytochemical applications of specific antisera raised against synthetic fragment peptides of mummichog gth subunits: examining seasonal variations of gonadotrophs (fsh cells and lh cells) in the mummichog and applications to other acanthopterygian fishes. *General and Comparative Endocrinology*, **132**(1): 35-45, https://doi.org/10.1016/S0016-6480(03)00037-6.

Weltzien F A, Andersson E, Andersen Ø et al. 2004. The brain-pituitary-gonad axis in male teleosts, with special emphasis on flatfish (*Pleuronectiformes*). *Comparative Biochemistry and Physiology Part A*: *Molecular & Integrative Physiology*, **137**(3): 447-477, https://doi.org/10.1016/j.cbpb.2003.11.007.

Weltzien F A, Hildahl J, Hodne K et al. 2014. Embryonic development of gonadotrope cells and gonadotropic hormones-lessons from model fish. *Molecular and Cellular Endocrinology*, **385**(1-2): 18-27, https://doi.org/

10.1016/j.mce.2013.10.016.

Weltzien F A, Norberg B, Helvik J V et al. 2003. Identification and localization of eight distinct hormone-producing cell types in the pituitary of male Atlantic halibut (*Hippoglossus hippoglossus* L.). *Comparative Biochemistry and Physiology Part A*: *Molecular & Integrative Physiology*, **134**(2): 315-327, https://doi.org/10.1016/S1095-6433(02)00266-0.

Yoshie S, Honma Y. 1978. Experimental demonstration of the cell types in the adenohypophysis of the gobiid fish, *Rhinogobius brunneus*. *Archivum Histologicum Japonicum*, **41**(2): 129-140, https://doi.org/10.1679/aohc1950.41.129.

Zhang Z W, Lau S W, Zhang L L et al. 2015. Disruption of zebrafish follicle-stimulating hormone receptor (*fshr*) but not luteinizing hormone receptor (*lhcgr*) gene by TALEN leads to failed follicle activation in females followed by sexual reversal to males. *Endocrinology*, **156**(10): 3747-3762, https://doi.org/10.1210/en.2015-1039.

Zhu X Y, Gleiberman A S, Rosenfeld M G. 2007. Molecular physiology of pituitary development: signaling and transcriptional networks. *Physiological Reviews*, **87**(3): 933-963, https://doi.org/10.1152/physrev.00006.2006.

Electronic supplementary material

Supplementary material (Supplementary Table S1 and Figs.S1–S2) is available in the online version of this article at https://doi.org/10.1007/s00343-022-2250-7.